Electronic Supplementary Material (ESI) for ChemComm.

Supporting Information

Selective Cytotoxicity and Luminescence Imaging of Cancer Cells With A Dipicolinato-based Eu^{III} complex

Jorge H.S.K. Monteiro,[a, b] Daisy Machado,[c] Luciana M. de Hollanda,[c] Marcelo Lancellotti,[c] Fernando A. Sigoli,[a,] * Ana de Bettencourt-Dias[b,] *

a - Institute of Chemistry, University of Campinas, Campinas, São Paulo, Brazil
b - Department of Chemistry, University of Nevada, Reno, NV 89557
c - Institute of Biology, University of Campinas, Campinas, São Paulo, Brazil

Table of Contents

Experimental section

All commercially obtained reagents were of analytical grade and were used as received. Solvents were dried by standard methods. The stock solution of europium(III) chloride was prepared by dissolving the chloride salt in water. The concentration of the metal was determined by complexometric titration with EDTA (0.01 M) using xylenol orange as indicator.[1]

NMR spectra were recorded on Varian 400 and 500 MHz spectrometers with chemical shifts reported (δ, ppm) against tetramethylsilane (TMS) or sodium 2,2-dimethyl-2-silapentane-5-sulfonate (DSS). Electrospray ionization mass spectra (ESI-MS) were collected in positive or negative mode on a Waters Micromass ZQ quadrupole in the low-resolution mode for the ligands and in a Waters model XEVO in the high-resolution mode for the metal complexes with a QTOF analyzer. The FT-IR absorption spectra were recorded on a Nicolet 6700 FT-IR spectrometer in ATR mode with solid samples.

Ligand synthesis. The ligands were synthesized using standard methods or according to modified literature procedures, as shown in Scheme S1.[2-4]

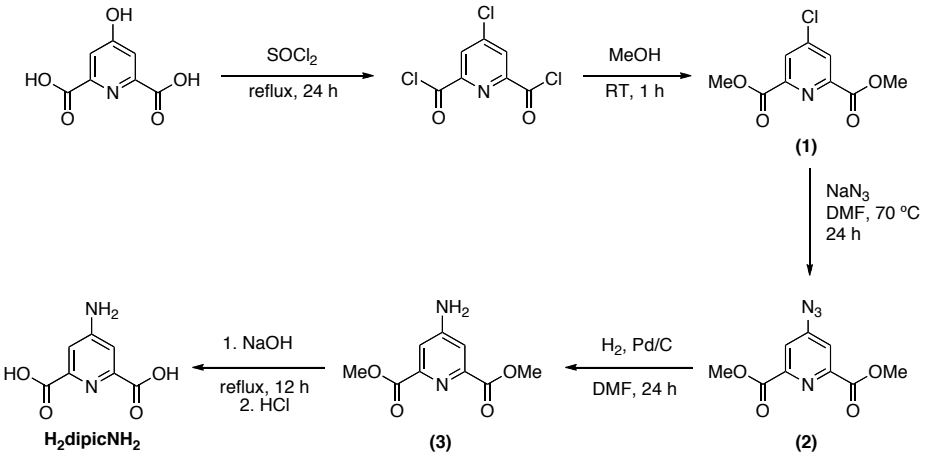

Scheme S1. Synthesis of H_2dipicNH_2.

Synthesis of dimethyl-4-chloropyridine-2,6-dicarboxylate (**1**).[2] 3.00 g (16.4 mmol) chelidamic acid monohydrate was added to 10 ml $SOCl_2$ with 1 drop DMF. The white suspension was refluxed for 24 h to yield a green-yellow solution. The $SOCl_2$ was removed under reduced pressure, 12 ml methanol was added under cooling, and the system was stirred for 1 h at RT. The excess methanol was removed under reduced pressure, the residue dissolved in chloroform and washed with water (2x) and brine (2x). The organic phases were dried over Na_2SO_4, filtered and the solvent removed under reduced pressure to yield 3.08 g (82%) of a white solid.

^{1}H-NMR ($CDCl_3$, 400 MHz): 8.30 (s, 2H, py); 4.04 (s, 6H, CH_3) ppm.

$^{13}C\{^{1}H\}$-NMR ($CDCl_3$, 126 MHz): 164.07; 149.38; 146.80; 128.28; 53.46 ppm.

Synthesis of dimethyl-4-azidopyridine-2,6-dicarboxylate (**2**).[3] 3.00 g (13.1 mmol) dimethyl-4-chloropyridine-2,6-dicarboxylate **1** was dissolved in DMF and 8.49 g (131 mmol) NaN_3 was added to yield a yellow suspension. The suspension was stirred at 70 ºC for 24 h, poured into water at 0 ºC and stirred vigorously for some minutes to yield 1.81 g (57%) of a light yellow solid, which was filtered and washed with cold water.

^{1}H-NMR (DMSO-d_6, 400 MHz): 7.87 (s, 2H, py); 3.92 (s, 6H, CH_3) ppm.

$^{13}C\{^{1}H\}$-NMR (DMSO-d_6, 126 MHz): 165.29; 151.71; 149.02; 118.58; 53.03 ppm.

Synthesis of dimethyl-4-aminopyridine-2,6-dicarboxylate (**3**).[4] 2.00 g (8.5 mmol) of **2** and 300 mg Pd/C (10%) were suspended in DMF to yield a black suspension, which was vigorously stirred at RT while purging with hydrogen for 24 h. The intermediate was used in the next step without further purification.

^{1}H-NMR (DMSO-d_6, 400 MHz): 7.36 (s, 2H, py); 6.72 (br, 2H, NH_2); 3.84 (s, 6H, CH_3) ppm.

Synthesis of 4-aminopyridine-2,6-dicarboxylic acid - H_2dipicNH_2. 8 mL 2.5 M NaOH was added to a suspension of **3**. The mixture was refluxed for 6 h and then allowed to cool to RT. The suspension was filtered and the pH of the solution adjusted to ~ 2 by slowly adding 10 % $HCl_{(aq)}$. The solid was filtered and washed with cold water to yield 800 mg (71%) of a white solid.

^{1}H-NMR (DMSO-d_6, 400 MHz): 7.35 (s, 2H, py); 7.07 (br, 2H, NH_2) ppm.

^{13}C-NMR (D_2O, pH >7, 126 MHz): 173.52; 156.05; 153.80; 110.73 ppm.

ESI-MS: $[M+Na^+]^-$ m/z 203 (exp.) 203 (calc.).

Synthesis of the metal complexes.[5] Ln_2O_3 (Ln = La^{III}, Eu^{III}, Gd^{III} or Tb^{III}) was suspended in water and H_2dipicNH_2 was added in a 1:3 (Ln:L) stoichiometry. The suspension was stirred at 100 ºC for 1 h and then its pH adjusted to ~6 with K_2CO_3, Na_2CO_3, or Cs_2CO_3. A clear solution was obtained, filtered and the solution evaporated to dryness. Crystals suitable for X-ray diffraction of $[CsK_2(H_2O)_5(MeOH)][Gd(dipicNH_2)_3]$ **(A)** and $[CsNa_2(H_2O)_5(MeOH)][Eu(dipicNH_2)_3]$ **(B)** were obtained through dissolution in hot water of the metal complexes and slow diffusion of methanol.

$K_3[La(DipicNH_2)_3]$. Yield 0.116 g, 80 %. ESI-MS $[La(dipicNH_2)_2]^-$ m/z 498.93 (exp.) 498.94 (calc).

$K_3[Eu(dipicNH_2)_3]$. Yield 0.130 g, 82%. ESI-MS $[NaKEu(dipicNH_2)_3]^-$ m/z 754.91 (exp.) 754.93 (calc.).

$Cs_3[Eu(dipicNH_2)_3]$. Yield 0.158 g, 79%. ESI-MS $[NaCsEu(dipicNH_2)_3]^-$ m/z 848.85 (exp.) 848.87 (calc.).

$Cs_3[Gd(dipicNH_2)_3]$. Yield 0.154 g, 77%. ESI-MS $[Gd(dipicNH_2)_2]^-$ m/z 517.94 (exp.) 517.96 (calc.).

$K_3[Tb(dipicNH_2)_3]$. Yield 0.124 g, 83%. ESI-MS $[Tb(dipicNH_2)_2]^-$ m/z 518.96 (exp.) 518.94 (calc.).

$Cs_3[Tb(dipicNH_2)_3]$. Yield 0.161 g, 80%. ESI-MS $[NaKTb(dipicNH_2)_3]^-$ m/z 854.88 (exp.) 854.87 (calc.).

$M_3[Ln(dipicNH_2)_3]$. FT-IR (3500 – 550 cm^{-1}, ν / cm^{-1}): 3360 (ν_s(N – H)); 1640, 1585, 1543 ($\nu_a(COO^-)$ + ν(C=C) + ν(C=N)); 1350 $\nu_s(COO^-)$.

^{1}H-NMR (TRIS/DCl – D_2O, 500 MHz): $K_3[La(dipicNH_2)_3]$: 7.30 (s, py).

Photophysical characterization. 1×10^{-4} M solutions of the complexes were prepared in aqueous 0.1 M TRIS/HCl or D_2O TRIS/DCl buffer (pH ~7.4) and their purity assessed by high resolution mass spectrometry and lifetime measurements. The absorption spectra were measured on a Perkin Elmer Lambda 35 spectrometer. Emission and excitation spectra of the complexes were obtained at ~77 K and ~298 K, respectively, on a Horiba Jobin Yvon Fluorolog-3 fluorimeter equipped with excitation (1200 gr/mm, blazed at 330 nm) and emission (1200 gr/mm, blazed at 500 nm) monochromators with an ozone-free 450 W xenon lamp as light source in the steady-state. The excitation spectra were obtained in the range 250-500 nm. The emission spectra were measured in the 400-750 nm range with the emitted light collected at a 90º angle from the excitation light. All spectra were corrected for instrumental response. The excited state decay curves were obtained with a pulsed 150 W xenon lamp using a TCSPC system. The bandpass for the spectra and the decay curves was adjusted in order to get a signal with intensity around 10^6 cps. The ligand's singlet and triplet energy levels values were obtained at ~77 K by deconvolution of the fluorescence and phosphorescence spectra, respectively, into their Franck-Condon progression and are reported as the 0-0 transition.[6] The quantum yields ϕ_x of the samples were determined at 25.0 ± 0.1°C using the equation below.

$$\phi_x = \frac{A_{st} I_{st} E_x}{A_x I_x E_{st}} \times \phi_{st}$$

A_{st} and A_x are the absorbance at the excitation wavelength of the standard *st* and sample *x*, respectively; I_{st} and I_x are the intensities of the excitation spectra at the excitation wavelength, E_{st} and E_x are the integrated emission spectra and ϕ_{st} is the quantum yield of the standard. Standards for quantum yield measurements were $Cs_3[Eu(dipic)_3]$ (ϕ ~24 %) and $Cs_3[Tb(dipic)_3]$ (ϕ ~22 %) in 0.1 mol L^{-1} aqueous TRIS/HCl buffer solution (pH ~7.4).[7,8] The excitation wavelengths were chosen to ensure a linear relationship between the intensity of emitted light and the concentration of the absorbing/emitting species ($A \leq 0.05$). The number of coordinated water molecules (q) was determined through comparison of the emission lifetimes of Eu^{III} and Tb^{III} in water τ_{H2O} and deuterated water τ_{D2O}, using equation 1.[9]

$$q = A\left(\frac{1}{\tau_{H_2O}} - \frac{1}{\tau_{D_2O}} - B\right) \qquad (1)$$

A is 1.1 for Eu^{III} and 4.2 for Tb^{III} and B is 0.31 for Eu^{III} and 0 for Tb^{III}.

All data are the average of at least three independent measurements.

The speciation/molar fraction as a function of the concentration of the Eu^{III} complex (Figure S17) was determined using the emission lifetime values in aqueous 0.1 M TRIS/HCl buffer (pH ~7.4), as reported by Bünzli and co-workers.[7] To determine the stability constants, solutions of $K_2dipicNH_2$ and $EuCl_3$ with a wide range of stoichiometric ratios were prepared and the emission spectra obtained using λ_{exc} = 290 nm. Refinement of the stability constants was performed using the HypSpec2014 software.[10] The speciation graphs were generated using the HySS software.[11] Emission lifetimes were used to verify decomplexation of Eu^{III} in the presence of Ca^{II}, Zn^{II} or Fe^{III} (pH ~7.4, final physiologically relevant concentrations of 2, 0.3 and 1 mM, respectively).[12]

The intrinsic quantum yield ϕ_{Eu}^{Eu} was determined using equation 2.[13]

$$\phi_{Eu}^{Eu} = \frac{A_{rad}}{A_{tot}} \qquad (2)$$

A_{tot} is the total emission rate ($A_{tot} = k_R + k_{NR} = 1/\tau_{exp}$).

The sensitization efficiency (η_{sens}) was determined using equation 3.

$$\eta_{sens} = \frac{\phi_{Eu}^{L}}{\phi_{Eu}^{Eu}} \qquad (3)$$

ϕ_{Eu}^{L} is the efficiency or quantum yield of sensitized emission.

The distance donor-acceptor (R_L) was obtained using the LUMPAC software.[14]

X-ray crystallographic characterization. Crystal data, data collection, and refinement details for compounds $[CsK_2(H_2O)_5(MeOH)][Gd(dipicNH_2)_3]$ **(A)** and $[CsNa_2(H_2O)_5(MeOH)][Eu(dipicNH_2)_3]$ **(B)** are given in Table S1. Suitable crystals were mounted on a glass fiber and placed in a low temperature nitrogen stream. Data were collected on a Bruker SMART CCD area detector diffractometer equipped with a low-temperature device, using graphite-monochromated Mo-Kα radiation (λ = 0.71073 Å). Data were measured using a strategy combining ω and φ scan frames of 0.3° per frame and an acquisition of 10 or 20 s per frame. Multi-scan absorption corrections were applied. Cell parameters were retrieved using SMART[15] software and refined using SAINTPlus[16] software on all observed reflections. Data reduction and correction for Lp and decay were performed using the SAINTPlus[16] software. Absorption correction was applied using SADABS.[17] The structures were solved by direct methods and refined by least-square methods on F^2 using the SHELXTL[18] programming package. All non-hydrogen atoms were refined anisotropically. The hydrogen atoms were added geometrically and their parameters constrained to the parent site. For complexes with coordinated water molecules and water molecules of crystallization, hydrogen atoms could not be located on the difference map, could not be added geometrically, and have been omitted, although the formulas are correct. X-ray crystallographic information files can be found free of charge via www.ccdc.ca.ac.uk/cont/retrieving.html (or from the CCDC, 12 Union Road, Cambridge CB2 1EZ, U.K.; fax + 44 1223 336033; email data_request@ccdc.cam.ac.uk). CCDC 1534740 corresponds to the structure of **A**, and CCDC 1534741 correponds to the structure of **B**.

Table S1. Details of the X-ray crystallographic characterization of compounds **A** and **B**.

Compound	**A**	**B**
CCDC number	1534740	1534741
Formula	$C_{22}H_{26}CsGdK_2N_6O_{18}$	$C_{22}H_{26}CsEuN_6Na_2O_{17}$
M/g mol^{-1}	1030.85	977.34
Crystal system	Monoclinic	Monoclinic
Space group	P21/n	P21/n
a/Å	9.4903(1)	9.5125(2)
b/Å	24.0900(3)	24.0522(6)
c/Å	14.2494(2)	14.1809(3)
α/^{o}	90	90
β/^{o}	104.2850(7)	104.6492(15)
γ/^{o}	90	90
V/Å^3	3156.99(7)	3139.07(12)
T/K	100	101
Z	4	4
D_c/g cm^{-3}	2.169	2.068
μ(Mo-Kα)/mm^{-1}	3.59	3.26
Independent reflections, R_{int} [$F_o \geq 4\sigma(F_o)$]	9200, 0.064	11895, 0.075
Reflections collected	52735	40112
Data/restraints/parameters	9200 / 0 / 461	11895 / 0 / 453
Goodness-of-fit on F^2	1.05	1.03
R_1, wR_2 (all data)	0.081, 0.257	0.071, 0.181
Largest diff. peak and hole/e Å^{-3}	3.715 and -6.726	2.993 and 3.821

Cell culture. NIH/3T3 (ATCC® CRL-1658™, mouse fibroblasts) and PANC-1 (ATCC® CRL-1658™, human epithelioid carcinoma) cell lines were obtained from American Type Culture Collection (ATCC; Manassas, VA). The NG97 cell line derived from a human astrocytoma grade III, which started to develop and express important phenotypical characteristics of an astrocytoma grade IV, was kindly provided by Dr. Liana Verinaud. All cell lines were routinely grown in RPMI supplemented with 10% fetal bovine serum (FBS) and antibiotics (100 μg mL^{-1} penicillin, 10 μg mL^{-1} streptomycin) in a humidified incubator with 5% carbon dioxide, at 37 ºC. The cells (NIH/3T3, PANC-1 and NG97) were plated in 96 well plates and 24 h later the cells were pre-treated with complexes (12.5 – 200 μg mL^{-1}), the Ln^{III} chlorides and triflates salts (12.5 – 200 μg mL^{-1}) or $H_2dipicNH_2$ (12.5 – 200 μg mL^{-1}) for 48 h.

Cell viability studies. The cell viability was analyzed by MTT reduction assay. The medium was removed from the cells and 100 mL of thiazol blue tetrazolium bromide (MTT) solution (0.5 mg mL^{-1} in FBS free culture medium) was added to each well. After incubation for 2 h at 37 ºC, the MTT solution was removed and the formazan crystals were dissolved in 100 mL of ethanol. The plate was shaken for 5 minutes on a plate shaker and the absorbance was measured at 570 nm in a spectrophotometer ELx800 Absorbance Microplate Reader (BioTek, USA).[19] The measured absorbance at λ = 570 nm was normalized to % of control. This value was calculated by multiplying the absorbance of a treated well by 100 and dividing it by the average absorbance of a control well, which was considered 100%. The experiment was conducted in triplicate and the results are expressed as the mean ± standard deviation.[20-22] Data from each assay were analyzed statistically by ANOVA. Multiple comparisons among groups were determined with the Tukey test. Differences were considered significant when the p value was less than 0.05.

Blood-brain barrier (BBB) test.[23, 24] Endothelial HUVEC cells (ATCC® CRL-1730™) were plated in a 24 well plate with 3.0 μm pore size trans-well cell culture inserts and allowed to grow until 100% confluent. Next, the upper part of the trans-well medium was replaced by the medium with 200 μg mL^{-1} $K_3[Eu(dipicNH_2)_3]$ and put in a 24 well plate containing NG97 cells coverslips. After 24 h the coverslips were fixed with 4% paraformaldehyde solution for 20 min at RT, washed with PBS (phosphate buffer solution) and fixed with glycerol. The confocal microscope images of the NG97 fixed cells were obtained on a Zeiss LSM 780 system coupled to a Zeiss Axio observer Z.1 microscope and a diode laser as the excitation source (405 ± 10 nm). The pinhole was adjusted to 1 airy unit for each channel for best signal/noise.

Cell microscopy images. The images of the NIH/3T3, NG97 and PANC-1 cells were obtained using the complex $K_3[Eu(dipicNH_2)_3]$ (200 μg mL^{-1}) as a luminescent dye on a Zeiss LSM 780 system coupled to a Zeiss Axio observer Z.1 microscope and a diode laser as the excitation source (405 ± 10 nm; $^5L_6 \leftarrow {}^7F_0$ transition of Eu^{III}). The pinhole was adjusted to 1 airy unit for each channel for best signal/noise.

Cell emission spectra. The emission spectra of the Eu^{III} complex in the cells, due to the small sample amounts, were acquired using a confocal T64000 Raman spectrometer system (Jobin-Yvon) using the single mode setup and a grating of 1800 gr/mm. A laser (488 nm, 1.8 mW) focused on a ~1 mm spot with a 50× focal objective lens (Leica PL Fluotar, NA = 0.55) was used to excite the cells ($^5D_2 \leftarrow {}^7F_2$ transition of Eu^{III}). For all measurements, the laser exposure time was 30 s without any accumulation and the emission was detected by a liquid N_2 cooled CCD.

[1]H-NMR spectra

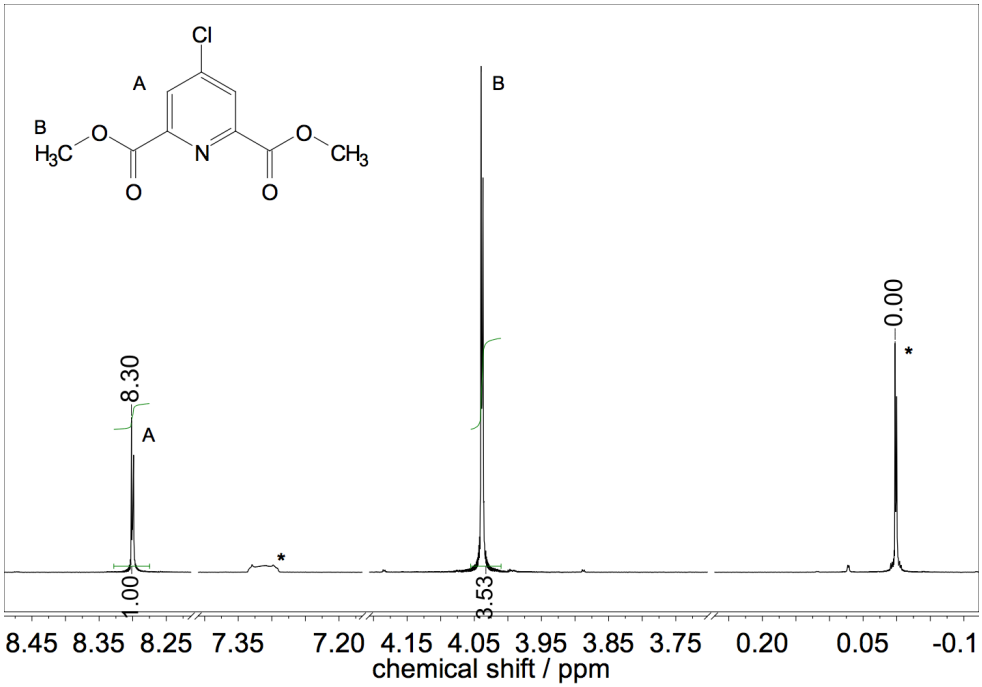

Figure S1. [1]H-NMR spectrum of dimethyl-4-chloropyridine-2,6-dicarboxylate (**1**) (*$CDCl_3$ 7.26 ppm; *TMS 0.00 ppm).

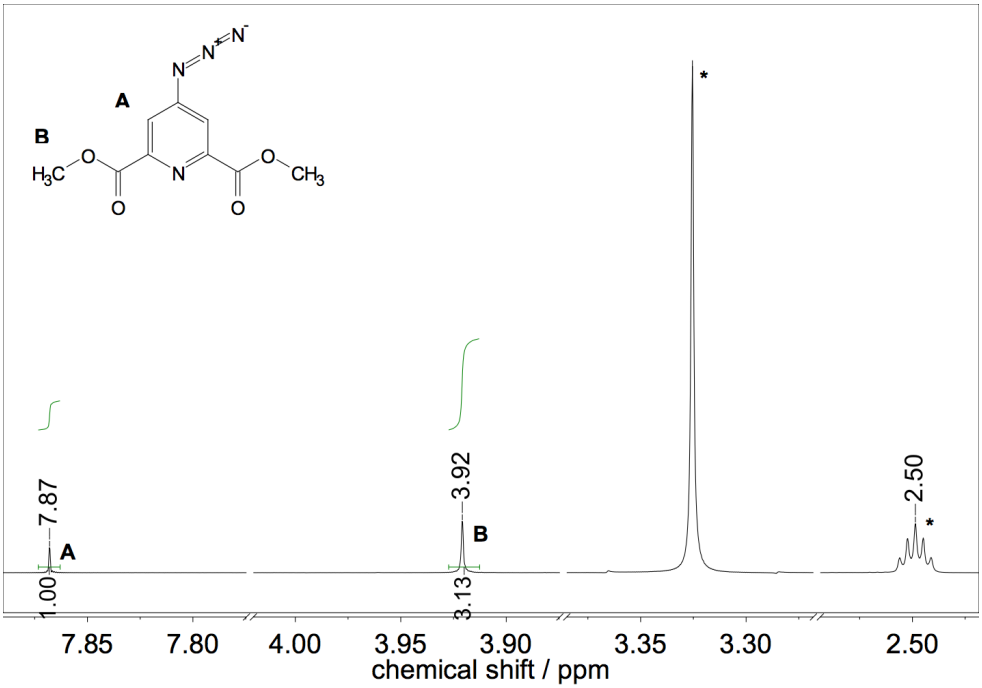

Figure S2. [1]H-NMR spectrum of dimethyl-4-azidopyridine-2,6-dicarboxylate (**2**) (*H_2O 3.33 ppm; *DMSO 2.50 ppm).

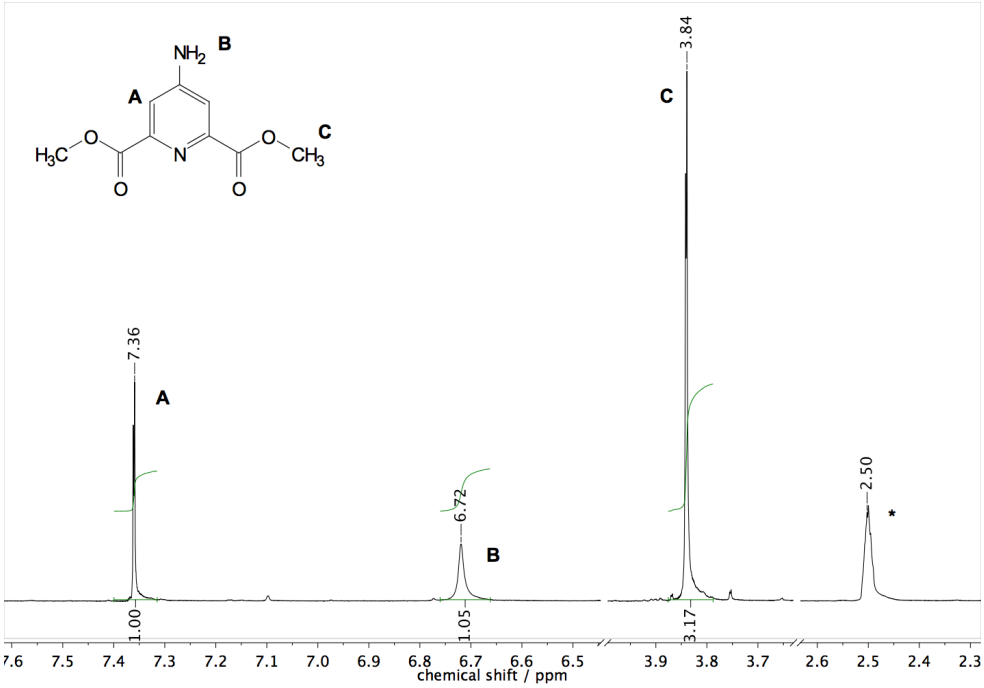

Figure S3. [1]H-NMR spectrum of dimethyl-4-aminopyridine-2,6-dicarboxylate (**3**) (*DMSO 2.50 ppm).

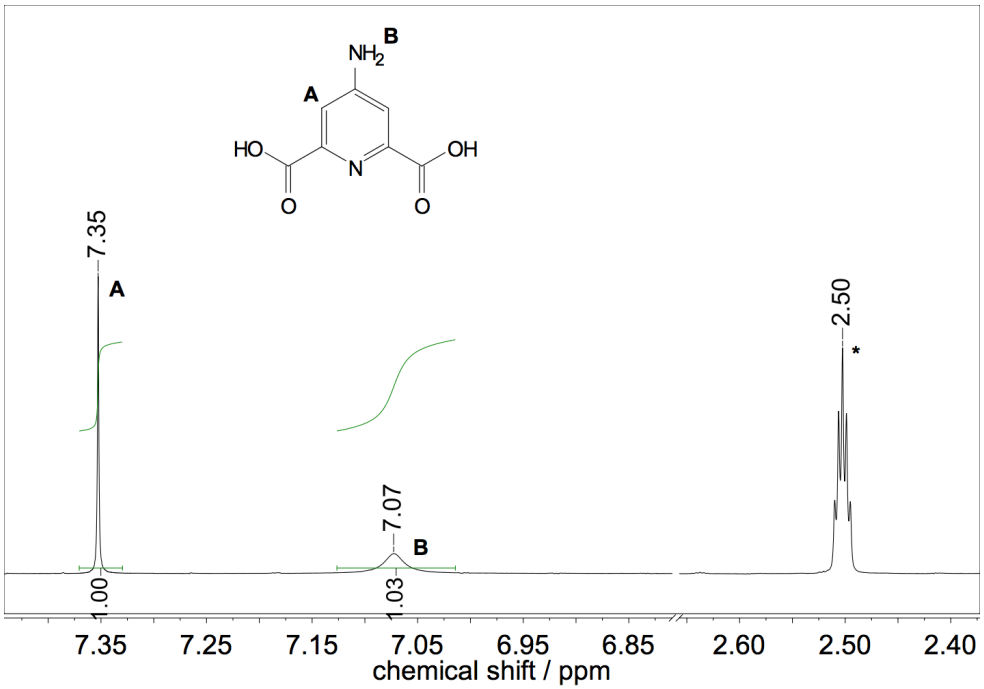

Figure S4. [1]H-NMR spectrum of 4-aminopyridine-2,6-dicarboxylic acid (**H_2dipicNH_2**) (*DMSO 2.50 ppm).

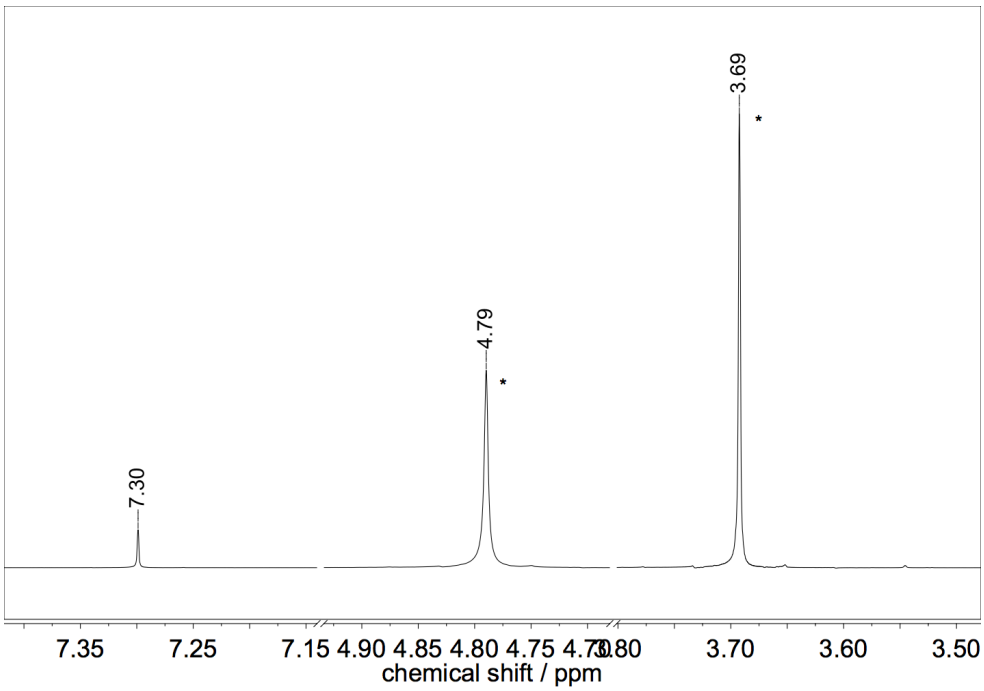

Figure S5. ^{1}H-NMR spectrum of $K_3[La(dipicNH_2)_3]$ (*D_2O 4.79 ppm; *CH_2(TRIS) 3.69 ppm).

^{13}C-NMR spectra

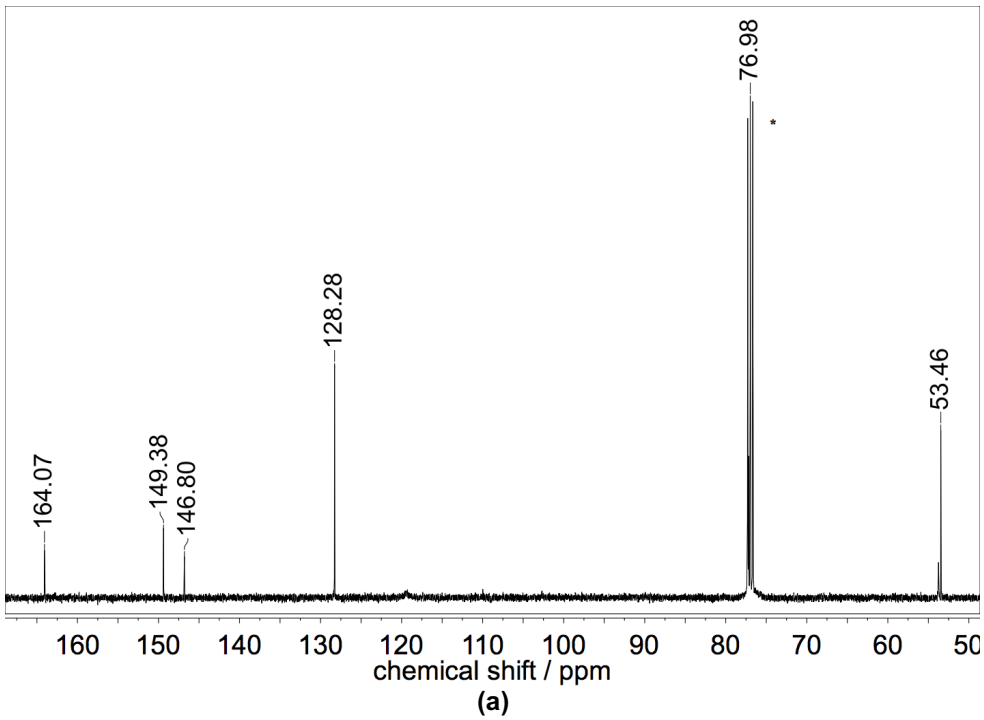

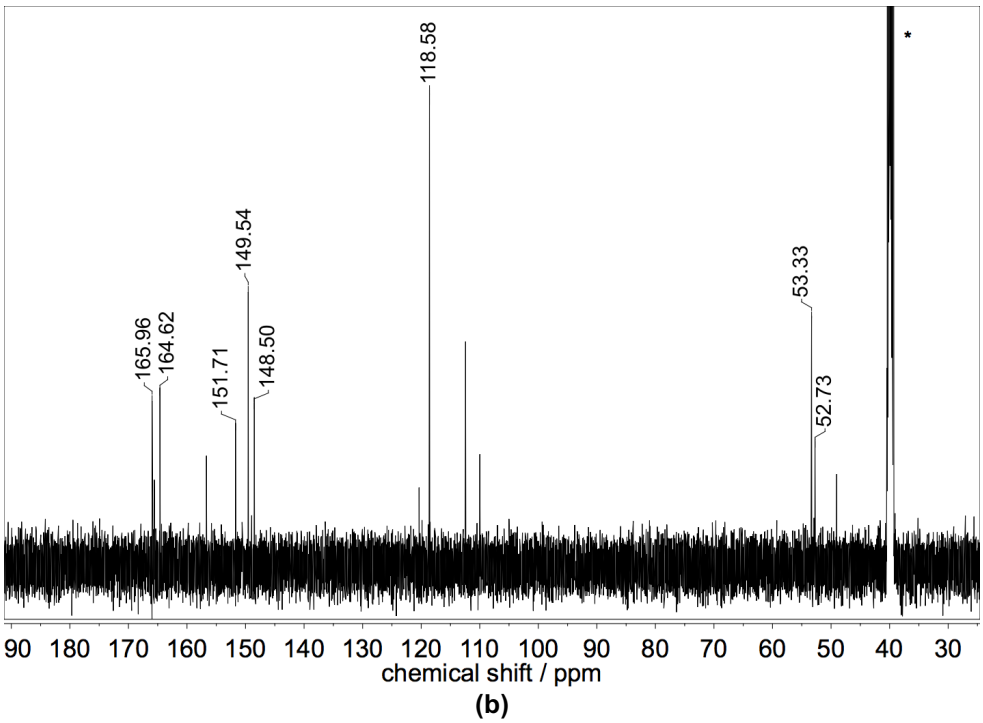

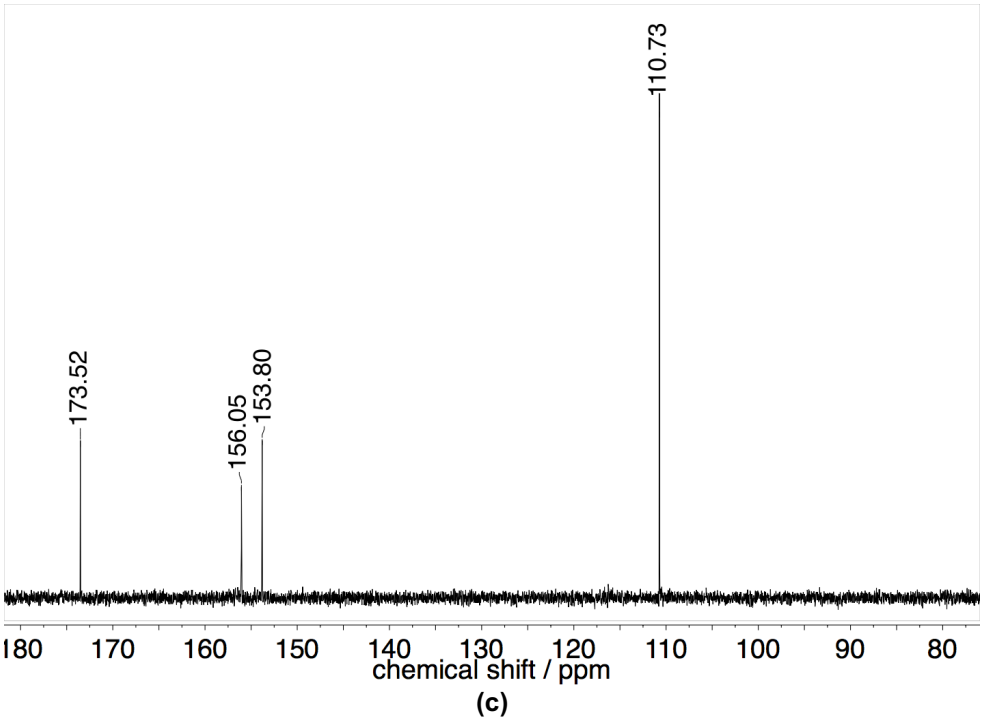

Figure S6. ^{13}C-NMR spectra of (a) **1**, (b) **2** and (c) **H_2dipicNH_2**.

ESI-mass spectra

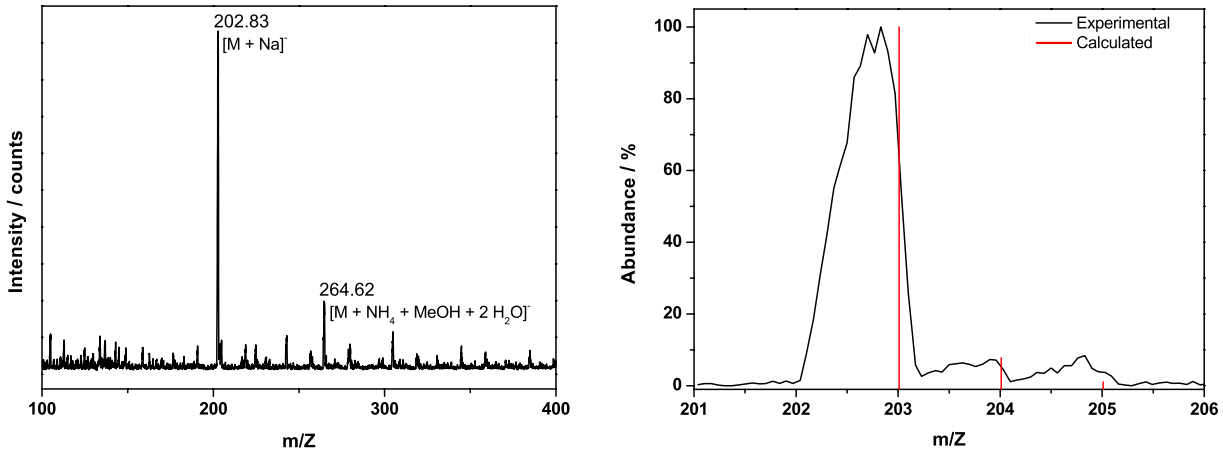

(a) (b)

Figure S7. (a) ESI-MS of 4-aminopyridine-2,6-dicarboxylic acid (**H_2dipicNH_2**). (b) Isotope pattern.

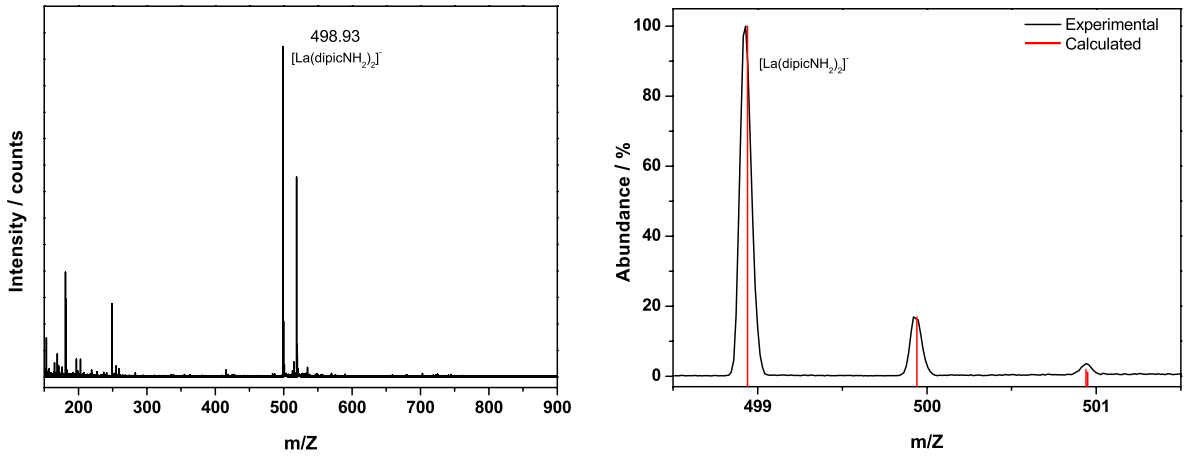

(a) (b)

Figure S8. (a) ESI-MS of $K_3[La(dipicNH_2)_3]$. (b) Isotope pattern.

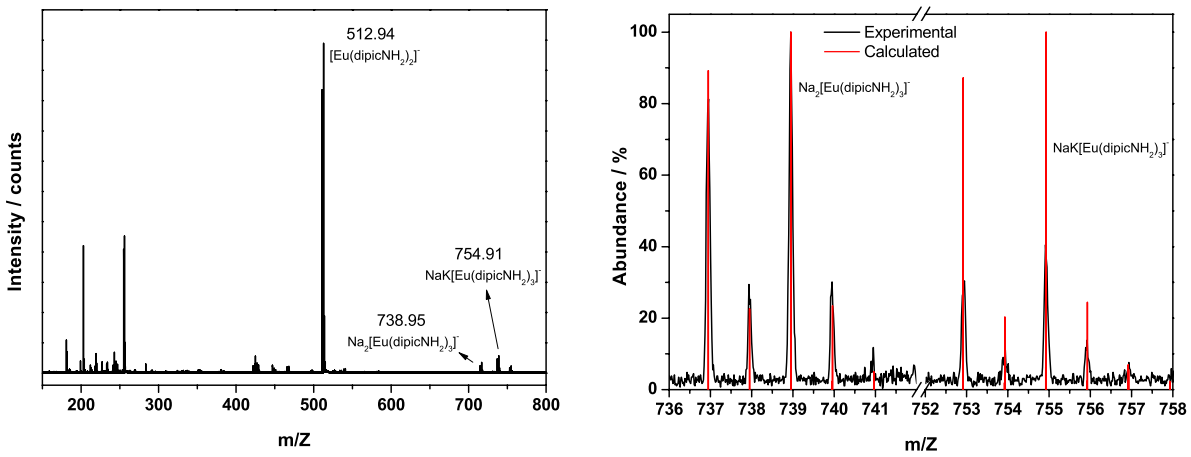

(a) **(b)**

Figure S9. (a) ESI-MS of $K_3[Eu(dipicNH_2)_3]$. (b) Isotope pattern.

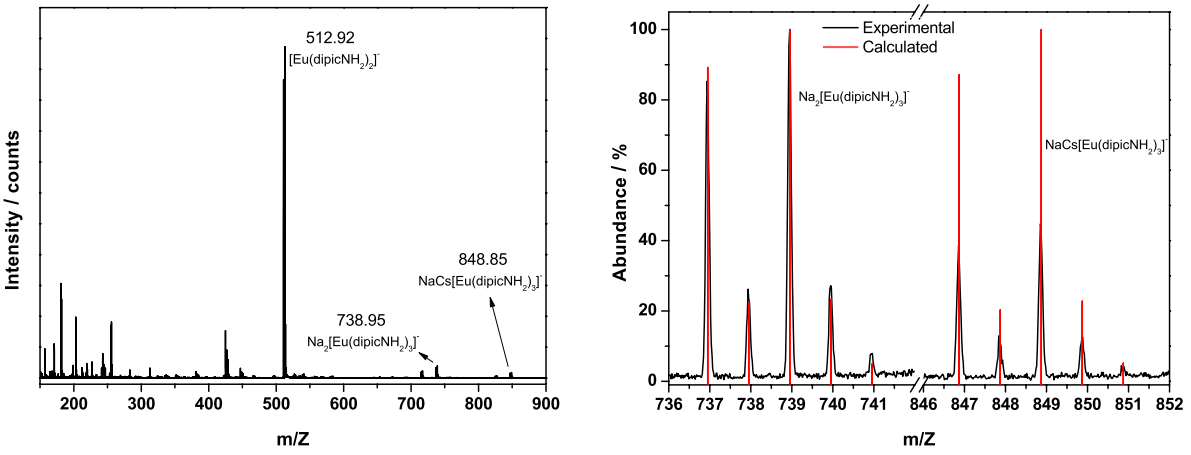

(a) **(b)**

Figure S10. (a) ESI-MS of $Cs_3[Eu(dipicNH_2)_3]$. (b) Isotope pattern.

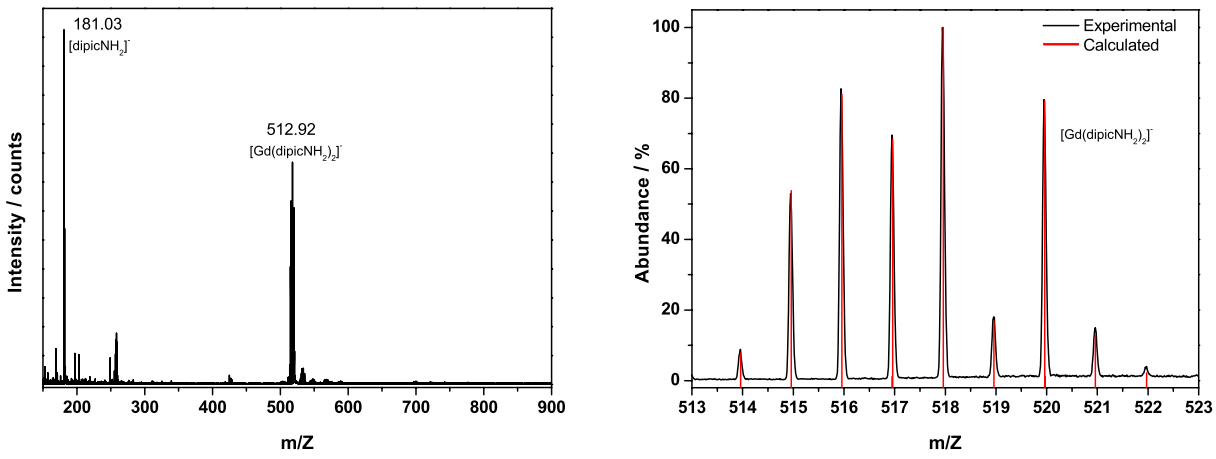

(a) (b)

Figure S11. (a) ESI-MS of $Cs_3[Gd(dipicNH_2)_3]$. (b) Isotope pattern.

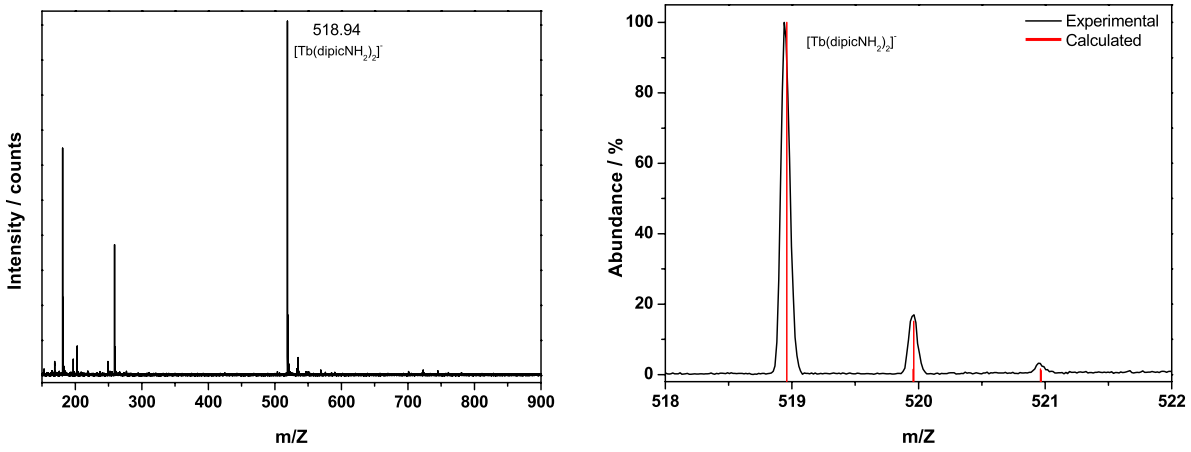

(a) (b)

Figure S12. (a) ESI-MS of $K_3[Tb(dipicNH_2)_3]$. (b) Isotope pattern.

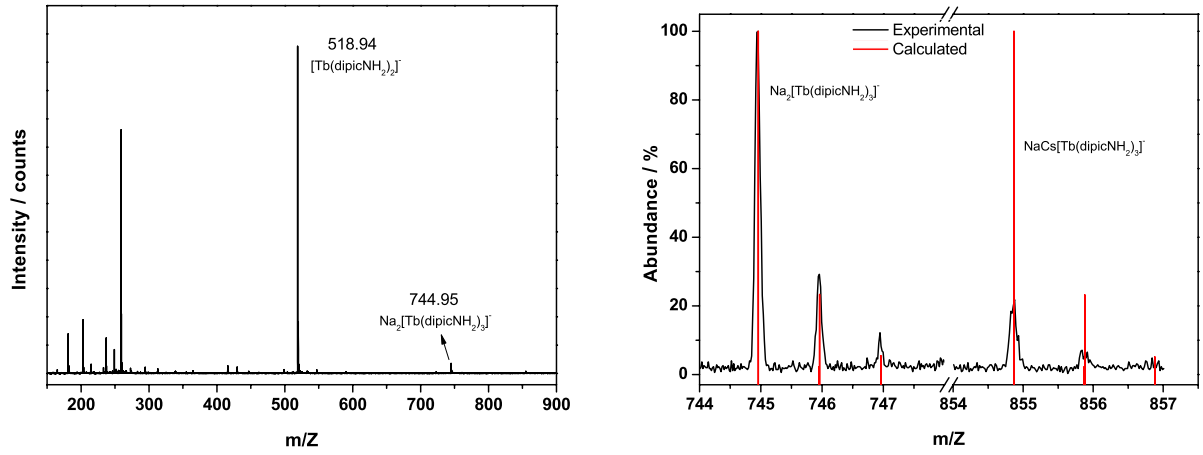

(a) (b)

Figure S13. (a) ESI-MS of $Cs_3[Tb(dipicNH_2)_3]$. (b) Isotope pattern.

FT-IR spectra

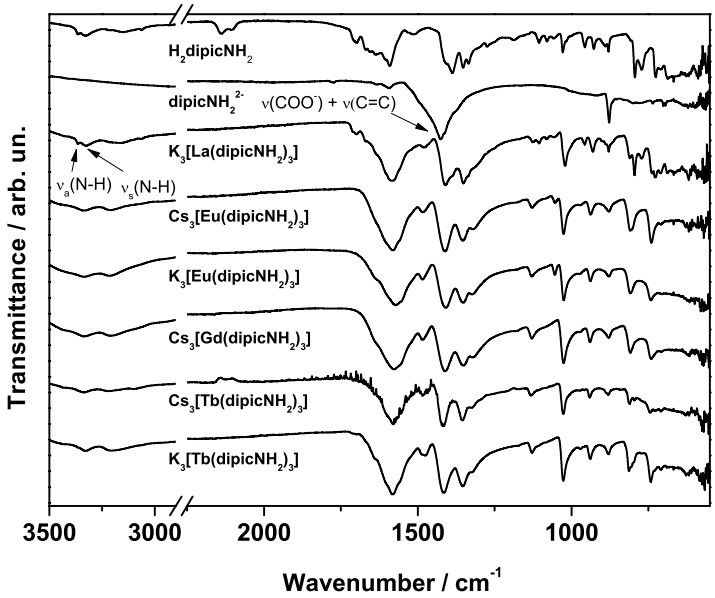

Figure S14. FT-IR spectra of the $H_2dipicNH_2$, its sodium salt ($dipicNH_2^{2-}$) and its Ln^{III} complexes.

Photophysical characterization of $M_3[Ln(dipicNH_2)_3]$ (M = K, Cs, Ln = Eu^{III}, Gd^{III})

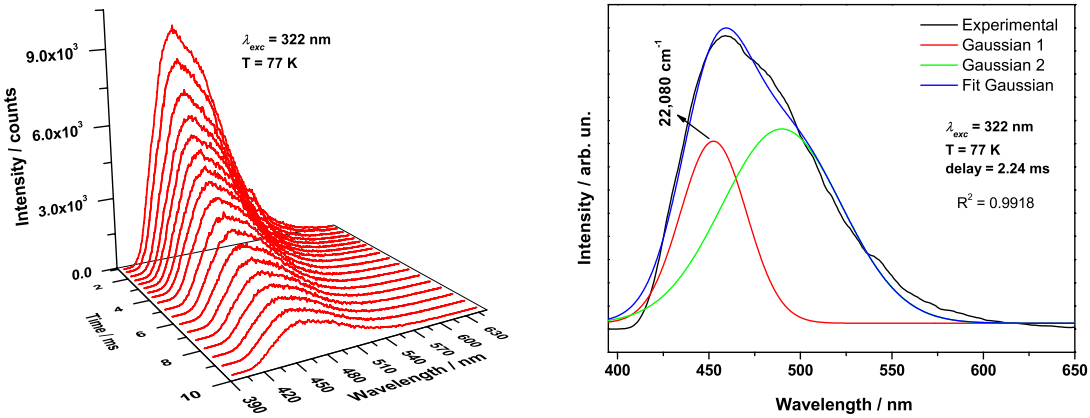

Figure S15. (a) Time-resolved phosphorescence spectra of $Cs_3[Gd(dipicNH_2)_3]$ at ~77 K. (b) Deconvolution of the phosphorescence band into its vibrational components.

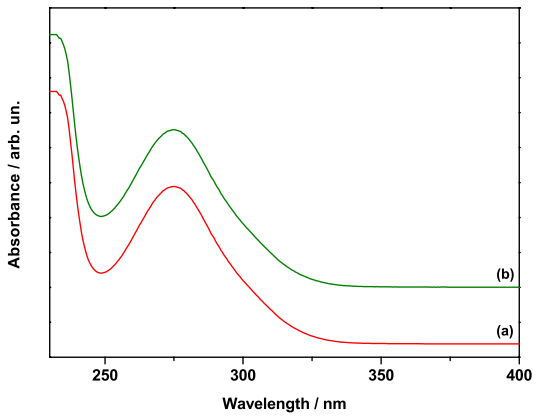

Figure S16. Absorption spectra of (a) $[Eu(dipicNH_2)_3]^{3-}$ and (b) $[Tb(dipicNH_2)_3]^{3-}$.

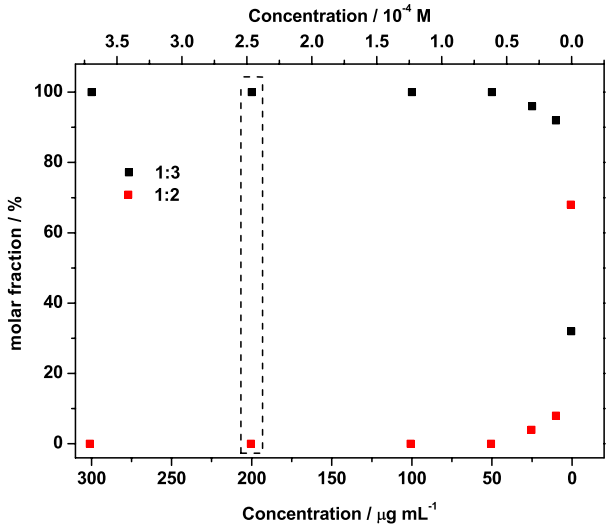

Figure S17. Proportion of 1:3 and 1:2 species in aqueous 0.1 M TRIS/HCl or D_2O TRIS/DCl buffer (pH ~7.4). for the $K_3[Eu(dipicNH_2)_3]$ complex.

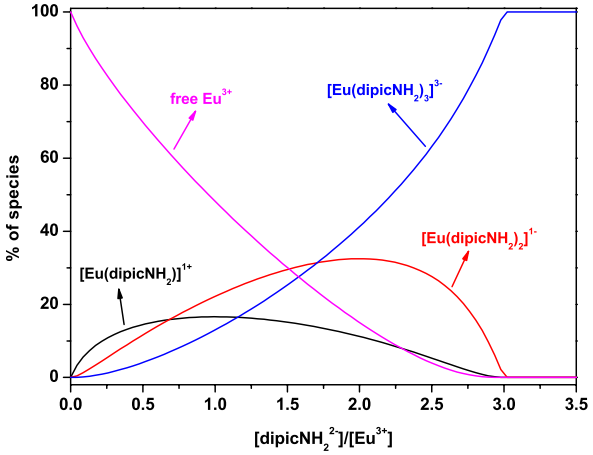

Figure S18. Speciation diagram showing percent formation of the various species as a function of the ratio $dipicNH_2^{2-}/Eu^{3+}$ in TRIS/HCl buffered aqueous solution (pH ~7.4).

Table S2. Emission lifetimes (τ) in the absence and presence of 2 mM Ca^{II}, 0.3 mM Zn^{II} and 1 mM Fe^{III}.

	$K_3[Eu(dipicNH_2)_3]$	Ca^{II}	Zn^{II}	Fe^{III}
τ / ms	1.27±0.01	1.26±0.01	1.25±0.01	1.24±0.01

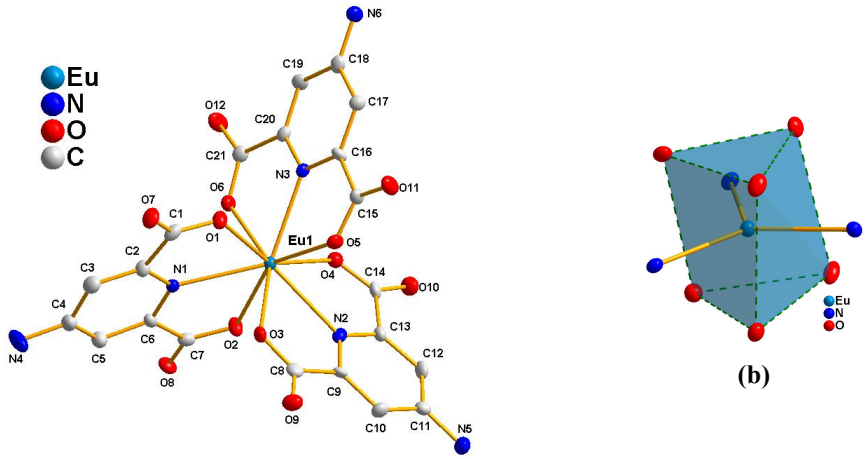

Figure S19. (a) Thermal ellipsoid plot at 50 % probability of $K_3[Eu(dipicNH_2)_3]$. (b) Coordination polyhedra around the Eu^{III} ion.

Table S3. Quantum yield (ϕ), intrinsic emission efficiency (ϕ_{Ln}^{Ln}), sensitization efficiency (η_{sens}), lifetime (τ), water molecules (q) in the first coordination sphere and distance donor-acceptor (R_L) obtained for the complexes in aqueous TRIS/HCl or TRIS/DCl buffered solutions (pH ~7.4).

Complexes	ϕ [%]	ϕ_{Ln}^{Ln} [%]	η_{sens} [%]	τ_{H2O} [ms]	τ_{D2O} [ms]	q	R_L [Å]
$Cs_3[Eu(dipicNH_2)_3]$	30±1	54	56	1.202±0.004	2.333±0.006	0.1	4.1257
$Cs_3[Tb(dipicNH_2)_3]$	24±1	-	-	1.465±0.003	1.796±0.003	0.5	-

Cell viability studies

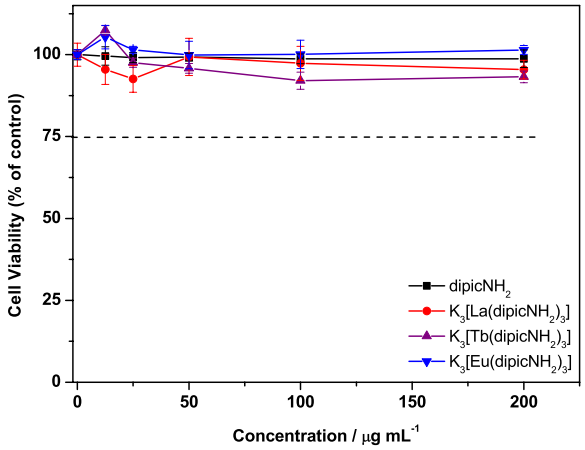

Figure S20. Cell viability of the ligand dipicNH$_2$ and its complexes after an incubation time of 48 h, determined by MTT assay, for NIH/3T3 cells.

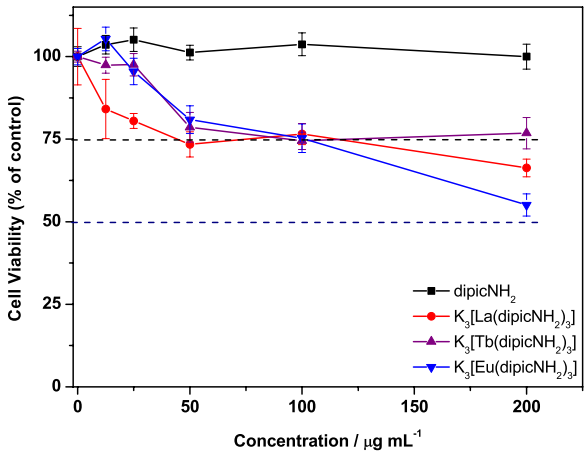

Figure S21. Cell viability of the ligand dipicNH$_2$ and its complexes after an incubation time of 48 h, determined by MTT assay, for NG97 cells.

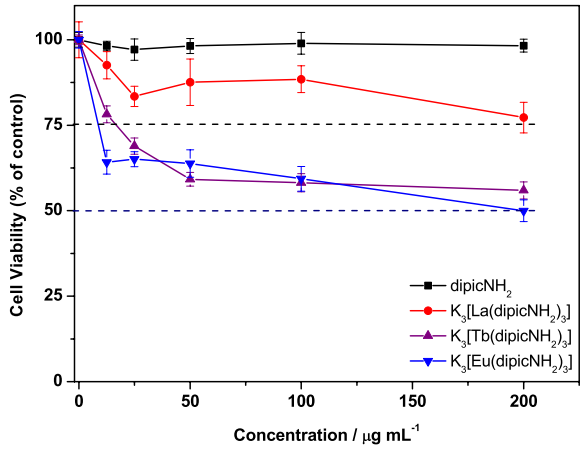

Figure S22. Cell viability of the ligand dipicNH$_2$ and its complexes after an incubation time of 48 h, determined by MTT assay, for PANC-1 cells.

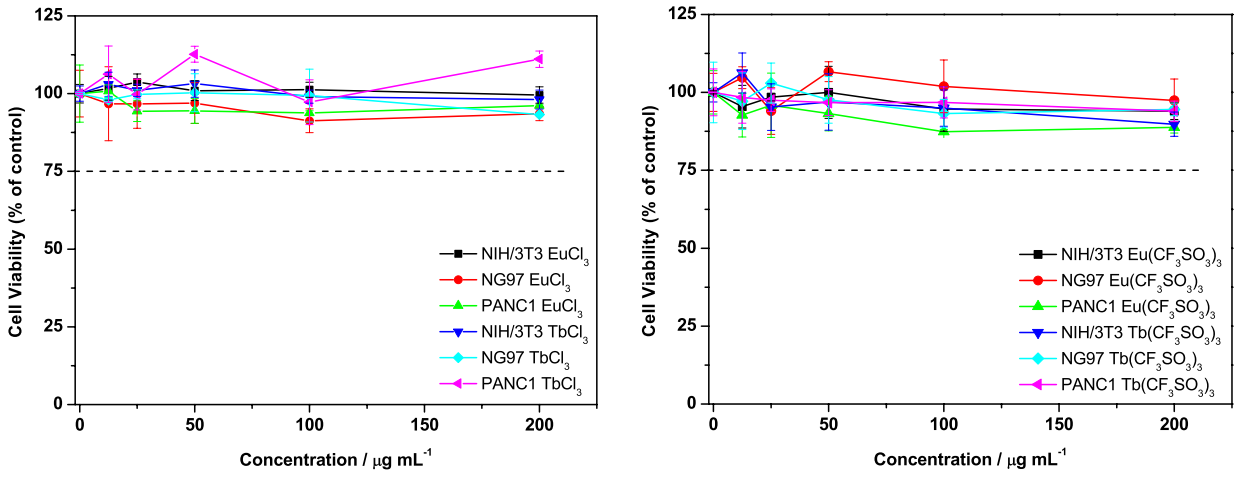

(a) **(b)**

Figure S23. Cell viability of the lanthanide salts, determined by MTT assay, for NIH/3T3, NG97 and PANC-1 cells after incubation for 48 h. (a) $EuCl_3$ and $TbCl_3$. (b) $Eu(CF_3SO_3)_3$ and $Tb(CF_3SO_3)_3$.

Confocal microscopy and emission spectroscopy of the incubated cells

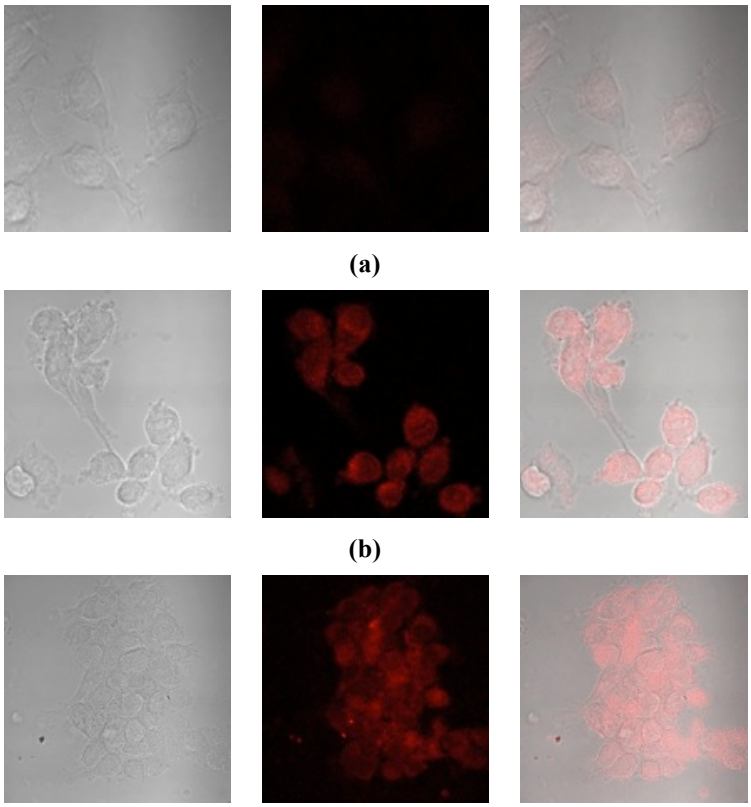

(a)

(b)

(c)

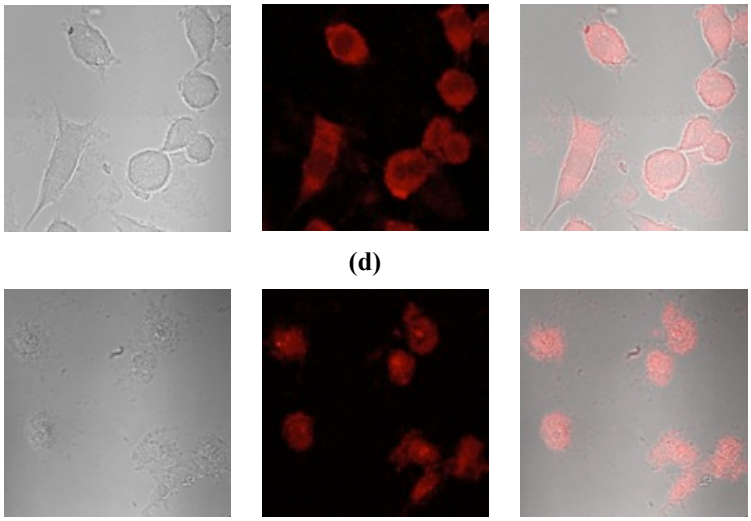

(d)

(e)

Figure S24. Confocal images of the NG97 cells in (a) absence of the complex and after incubation with the $K_3[Eu(dipicNH_2)_3]$ complex for (a) 3 h, (b) 6 h, (c) 12 h and (d) 24 h. In all images the first column is the bright field image, the second one is the luminescence and the third one is the overlay between the first and second columns.

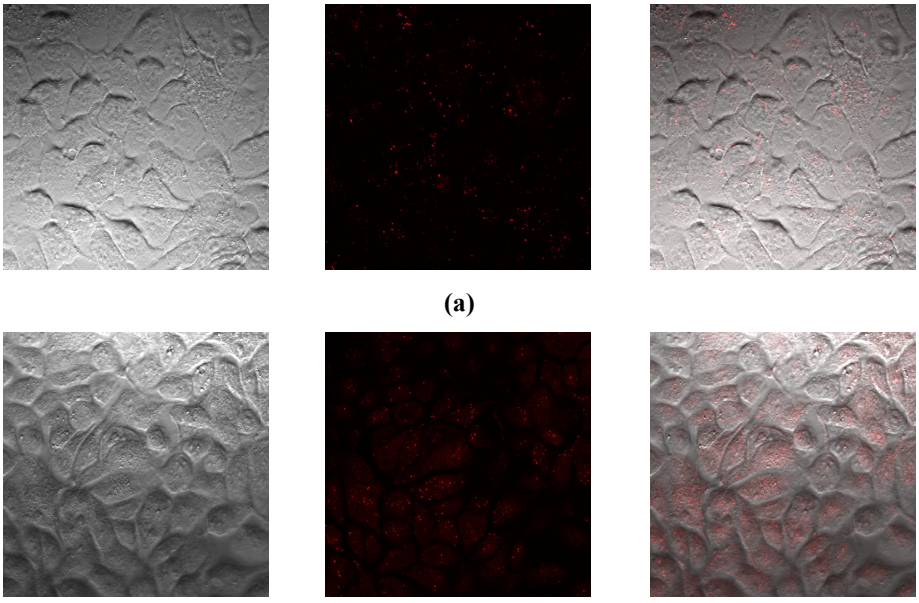

(a)

(b)

Figure S25. Confocal images of the PANC-1 cells in (a) absence of the complex and (b) after incubation with the $K_3[Eu(dipicNH_2)_3]$ complex for 24 h. In all images the first column is the bright field image, the second one is the luminescence and the third one is the overlay between the first and second columns.

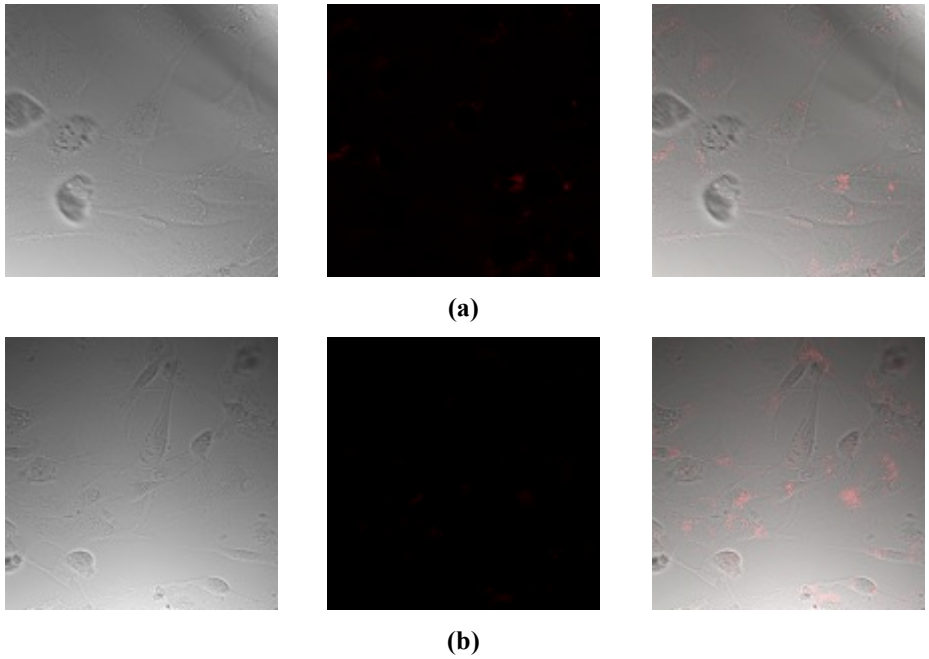

Figure S26. Confocal images of the NIH/3T3 cells in (a) absence of the complex and (b) after incubation with the $K_3[Eu(dipicNH_2)_3]$ complex for 24 h. In all images the first column is the bright field image, the second one is the luminescence and the third one is the overlay between the first and second columns.

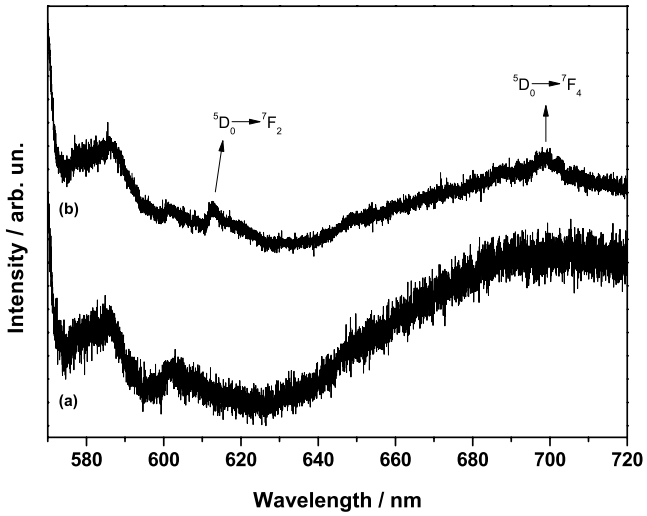

Figure S27. Emission spectra of the NIH/3T3 cells in (a) absence of the complex and (b) after incubation for 24 h.

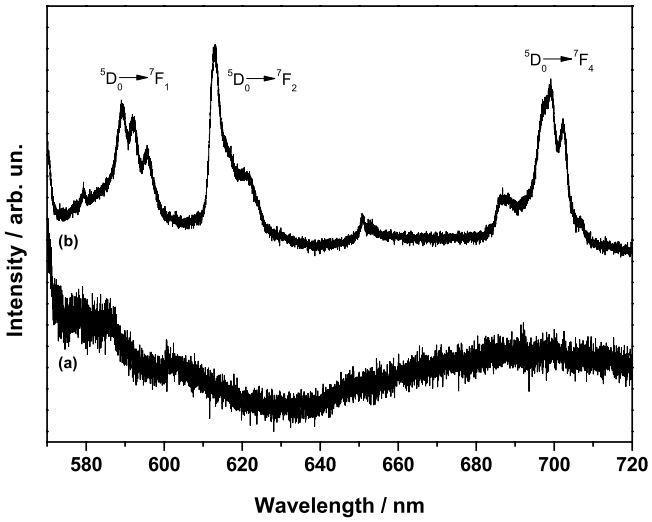

Figure S28. Emission spectra of the PANC-1 cells in (a) absence of the complex and (b) after incubation for 24 h.

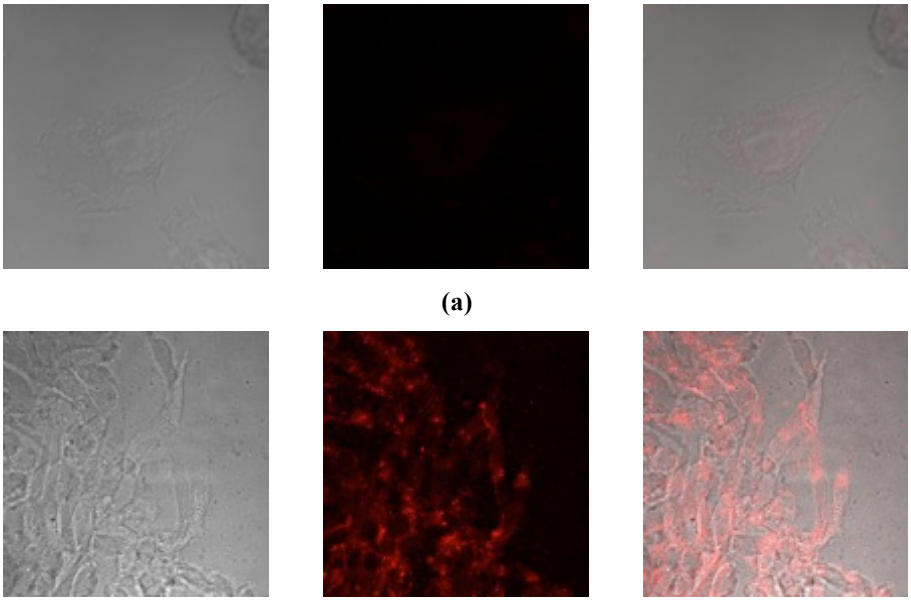

Figure S29. Confocal images obtained from the glass slide with NG97 cells after crossing the simulated barrier tests in (a) absence of the complex and (b) presence of the complex. The incubation time for all the experiments was 24 h.

References

1. J. Bassett, R. C. Denney, G. H. Jeffery and J. Mendham, *Vogel's Textbook of Quantitative Inorganic Analysis*, Longman Group, London, 4th ed. edn., 1978.
2. A. Picot, C. Feuvrie, C. Barsu, F. Malvolti, B. Le Guennic, H. Le Bozec, C. Andraud, L. Toupet and O. Maury, *Tetrahedron*, 2008, **64**, 399-411.

3. Z. E. A. Chamas, X. Guo, J. L. Canet, A. Gautier, D. Boyer and R. Mahiou, *Dalton Trans*, 2010, **39**, 7091-7097.
4. B. H. Huang, M. A. Prantil, T. L. Gustafson and J. R. Parquette, *J. Am. Chem. Soc.*, 2003, **125**, 14518-14530.
5. P. A. Brayshaw, J.-C. G. Bünzli, P. Froidevaux, J. M. Harrowfield, Y. Kim and A. N. Sobolev, *Inorg. Chem.*, 1995, **34**, 2068-2076.
6. G. A. Crosby, R. E. Whan and R. M. Alire, *The Journal of Chemical Physics*, 1961, **34**, 743-748.
7. A. S. Chauvin, F. Gumy, D. Imbert and J. C. G. Bünzli, *Spectrosc. Lett.*, 2004, **37**, 517-532.
8. *Spectrosc. Lett.*, 2007, **40**, 193-193.
9. R. M. Supkowski and W. D. Horrocks, *Inorg. Chim. Acta*, 2002, **340**, 44-48.
10. P. Gans, A. Sabatini and A. Vacca, *Talanta*, 1996, **43**, 1739-1753.
11. L. Alderighi, P. Gans, A. Ienco, D. Peters, A. Sabatini and A. Vacca, *Coord. Chem. Rev.*, 1999, **184**, 311-318.
12. U. Carpentieri, J. Myers, C. W. Daeschner and M. E. Haggard, *Biol. Trace Elem. Res.*, 1988, **16**, 165-176.
13. G. F. de Sá, O. L. Malta, C. de Mello Donegá, A. M. Simas, R. L. Longo, P. A. Santa-Cruz and E. F. da Silva, *Coord. Chem. Rev.*, 2000, **196**, 165-195.
14. J. D. L. Dutra, T. D. Bispo and R. O. Freire, *J. Comput. Chem.*, 2014, **35**, 772-775.
15. *Journal*.
16. *Journal*.
17. *Journal*.
18. *Journal*.
19. T. Mosmann, *Journal of Immunological Methods*, 1983, **65**, 55-63.
20. D. Machado, S. M. Shishido, K. C. Queiroz, D. N. Oliveira, A. L. Faria, R. R. Catharino, C. A. Spek and C. V. Ferreira, *PloS one*, 2013, **8**, e54269.
21. L. M. Hollanda, A. O. Lobo, M. Lancellotti, E. Berni, E. J. Corat and H. Zanin, *Mater Sci Eng C Mater Biol Appl*, 2014, **39**, 288-298.
22. H. Zanin, L. M. Hollanda, H. J. Ceragioli, M. S. Ferreira, D. Machado, M. Lancellotti, R. R. Catharino, V. Baranauskas and A. O. Lobo, *Mater Sci Eng C Mater Biol Appl*, 2014, **39**, 359-370.
23. *Brazil Pat.,* PI1103016-0, 2011.
24. J. Banerjee, Y. J. Shi and H. S. Azevedo, *Drug Discovery Today*, 2016, **21**, 1367-1386.